Available online at www.sciencedirect.com
SCIENCE DIRECT®
Vacuum 74 (2004) 19–28
VACUUM
SURFACE ENGINEERING, SURFACE INSTRUMENTATION & VACUUM TECHNOLOGY
www.elsevier.com/locate/vacuum

Alpha–gamma transition in RF capacitive discharge in low-pressure oxygen

V.A. Lisovskiy*, V.D. Yegorenkov

Kharkov National University, Svobody Sq. 4, Kharkov 61077, Ukraine

Abstract

We report the recorded current–voltage characteristics of a RF capacitive discharge in oxygen. Low-frequency oscillations of the plasma potential in a kilohertz frequency range are observed to accompany the transition of the discharge from a weak- (α-) to a strong-current (γ-) regime in the low-pressure range. The weak-current regime of the RF capacitive discharge is observed within the pressure range limited not only from the medium pressure side but also from the lower-pressure one. Electron temperature and plasma density are registered with a probe technique.

Keywords: Radio-frequency capacitive discharge; Low pressure; Probe; Negative ions

Introduction

Radio-frequency capacitive discharge in oxygen is widely used for processing semiconductor and polymer materials (etching, deposition, oxidizing, cleaning, etc.) [1–3]. A large number of experimental and theoretical papers studying the characteristics of this type of the discharge were published (see, e.g. [4–15]). But up to now the data are actually absent on the regimes of RF-capacitive discharge in oxygen and on the transition of the discharge from a weak-current (α-) to a strong-current (γ-) regime (α–γ transition). Therefore, it is vital to study the inner parameters of and regimes for the RF discharge in oxygen.

As is known [16–18], a RF discharge can exist in two different regimes: weak- (α-) and strong-current (γ-) ones. In α-regime the electrons acquire energy for ionising gas molecules in the RF field in the quasineutral plasma, the conductivity of the near-electrode sheaths is small, and the electron emission from the electrode surface does not play an essential role in the discharge sustainment. In γ-regime the electron avalanches develop in the near-electrode sheaths. The main ionisation of gas molecules by electrons in γ-regime occurs near the boundaries of the near-electrode sheaths, and the RF field in the quasineutral plasma cannot supply the electrons with sufficient energy for ionisation.

Ionisation instability can be observed in a gas discharge with negative ions [19,20]. In DC discharge in electro-negative gases such as CO_2, CO and O_2, the attachment-induced ionisation instability was observed by the authors of papers [21–23]. The paper [23] presented the most detailed theoretical treatment of the mechanism of this instability. The authors of this paper derived the criterion for the onset of this instability in plasma

*Corresponding author.
E-mail address: valeriy.lisovskiy@lptp.polytechnique.fr (V.A. Lisovskiy).

0042-207X/$ - see front matter
doi:10.1016/j.vacuum.2003.11.003

containing negative ions. This criterion was used by the authors of papers [13,24] for elucidating the nature of the instability they had observed in RF-capacitive discharge in oxygen.

Our paper reports the measurements of the RF current amplitude I_{rf} and of the phase shift φ between RF current and voltage as well as of the dependence of the active RF current $I_{rf}\cos\varphi$ on RF voltage amplitude U_{rf} (current–voltage characteristics of the RF discharge) for various values of oxygen pressure p. The extinguishing curve and the $\alpha-\gamma$ transition curve for the RF discharge are registered. It is observed that within the oxygen-pressure range $p \approx 26.6$–306 Pa the α–γ transition is accompanied by low-frequency oscillations of the plasma potential in the kilohertz frequency range. Electron temperature was measured with a single probe, and the axial profiles of the plasma density were also obtained.

Experimental conditions

Fig. 1 depicts the scheme of the experimental device used for registering the RF discharge characteristics. The section of a fused silica cylindrical tube (not shown in Fig. 1) with inner diameter of 100 mm vacuum-sealed on both ends with stainless-steel planar round electrodes 1 served as a discharge chamber. The puffing system 2 delivered oxygen into the chamber through small orifices in a grounded electrode. The chamber was evacuated through the orifices 3 in the same electrode. We used a thermoelectric gauge 4 for registering gas pressure from 0.133 Pa to the atmospheric one. The evacuation was accomplished with pre-vacuum and turbo molecular pumps permitting to achieve the limiting pressure of 2.7×10^{-4} Pa. One of the electrodes of the discharge chamber was grounded. The generator 5 delivered the RF voltage to another electrode via the matching box 6. The choke of $L_c = 4$ mH inductance switched across the electrodes outside the chamber removed the self-bias voltage.

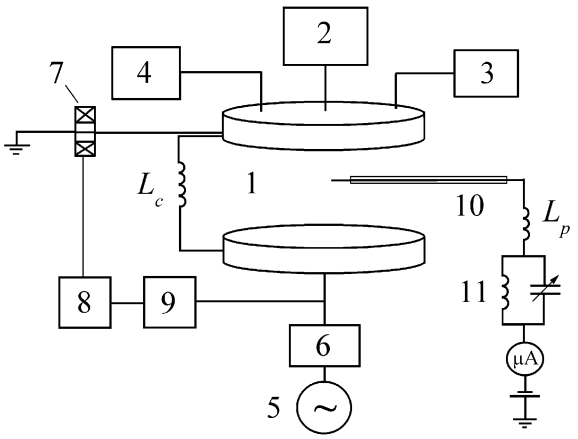

Fig. 1. Scheme of the experimental device.

The experiments were performed within the gas pressure range $p = 3.3$–666 Pa in the range of RF voltage amplitudes $U_{rf} \leqslant 700$ V and the RF field frequency $f = 13.56$ MHz. The distance between the electrodes was $L = 33$ mm. The amplitude of the RF current I_{rf} was measured with a Rogowski coil 7 located on the bus, which grounded one of the electrodes. The signal from the Rogowski coil was fed to the FK2-12 device 8. The signal from the capacitive divider 9 connected to the RF electrode was fed to another input of the FK2-12 device. The device for measuring the phase difference FK2-12 is capable of registering the amplitude of the RF signal having the frequency in the range of $f_1 = 1$ MHz–1 GHz and phase shift φ between two signals (in our case between RF voltage and RF current). In the absence of the discharge the registered phase shift value is $\varphi = 90^\circ = \pi/2$, i.e., we register only the displacement current. On igniting the RF discharge the active RF current appeared, the phase shift angle φ becomes less than $\pi/2$. The accuracy of measuring the phase shift angle with FK2–12 was 0.1°.

Electron temperature, plasma potential and density were registered with a single cylinder nichrome probe 10 (5.5 mm in length and 0.18 mm in diameter). We employed the resonance filter 11 consisting of a high-frequency choke and a variable capacitor tuned to the frequency f of the RF generator to prevent the RF current from penetrating the probe circuit. We also included an additional choke of $L_p = 10$ mH inductance to suppress the main frequency signal and its harmonics in the probe circuit. All three possible regimes of probe operation (collisionless, transitional and collisional) can be observed within the

pressure range studied. That is, at different values of gas pressure ions may traverse the near-probe sheath without collisions (this is observed under low gas pressure, $p<5$ Pa); they may experience several collisions (intermediate pressure) or multiple collisions ($p>100$ Pa). The plasma density (density of positive ions) n_i was calculated from the ion branch of the probe current I_{pr} and electron temperature T_e was measured according to the technique described in papers [25–27], permitting accurate determination of the density of positive ions from the probe current–voltage characteristic at arbitrary value of the gas pressure. Electron temperature T_e was determined from the linear sections of the probe current–voltage characteristics drawn to a semi-logarithmic scale, as well as from the second derivative of the probe current with respect to the DC voltage on the probe. The electron temperature T_e values measured with both techniques differed not more than by 10–20%. The presence of negative ions does not affect these techniques of measuring the electron temperature [28,29], what ensures the correct determination of T_e. To measure the second derivative d^2I_{pr}/dU_{pr}^2, the second harmonic technique was applied, i.e., the probe current was modulated with a low frequency voltage (with the frequency $f_{lf}\approx 1-3$ kHz), but the signal was registered at the frequency $2\,f_{lf}$. The set-up for measuring d^2I_{pr}/dU_{pr}^2 was described in paper [30]. Regretfully, this set-up did not permit to make correct measurements of the second derivative d^2I_{pr}/dU_{pr}^2 near the plasma potential, therefore we could not employ the technique for measuring the temperature T_n and density n_n of negative ions suggested in [28,29]. The same set-up based on the SK-54 spectrum analyser was used for recording the spectrum of low-frequency oscillations generated in the RF gas discharge.

Experimental results

Fig. 2 shows the RF current amplitude I_{rf} (Fig. 2a), the phase shift φ (Fig. 2b,c) and the active RF current $I_{rf}\cos(\varphi)$ (Fig. 2d) against the RF voltage at different oxygen pressure values. The RF generator supplied the RF voltage up to

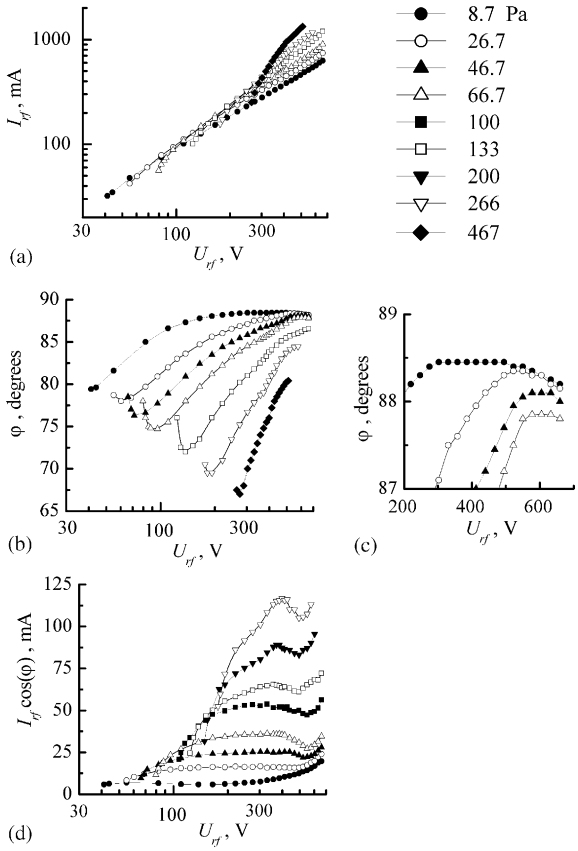

Fig. 2. RF current amplitude (a), phase shift angle (b, c) and active RF current (d) against RF voltage at different oxygen pressure values.

$U_{rf}\leqslant 700$ V, thus enabling us to study the characteristics of RF discharge in the weak-current regime, the $\alpha-\gamma$ transition and within a small section of the strong-current regime. Therefore, we observe a feebly expressed dogleg feature of the current–voltage characteristics (Fig. 2a) occurring when the discharge is passing to a strong-current regime. With the oxygen pressure fixed the curves in Fig. 2a possess an almost constant tilt which experiences strong changes only at the RF voltage value when the discharge is extinguished. However, we did not observe the normal current density feature [16] within the oxygen pressure range studied. It is clear from Fig. 2b,c that at low oxygen pressure ($p<13$ Pa) on increasing the RF voltage the phase shift angle increases, reaches a maximum and then decreases slowly in the

γ-regime. At higher oxygen pressures and low voltages U_{rf} the phase shift angle first decreases, passes through the minimum and then increases, reaches a maximum at the end of the $\alpha-\gamma$ transition, and then decreases in the strong-current regime of RF discharge. Fig. 2c gives a clear indication of the maximum through which the dependence of the phase shift φ on the RF voltage is passing.

The current–voltage characteristics of the discharge (Fig. 2d) possess a region with a negative differential conductivity. Similar effect was earlier observed in the RF capacitive discharge in argon [18,31]. In the weak-current regime of discharge on increasing the RF voltage the active RF current first grows, it decreases under the $\alpha-\gamma$ transition, reaches a minimum and grows quickly in the strong-current regime.

Let us realize exactly what change of the RF discharge parameters is expedient to take as a criterion of the $\alpha-\gamma$ transition. People often regard the value of the RF voltage U_{rf} at which a discontinuity in the derivative dI_{rf}/dU_{rf} is observed as the voltage value of the $\alpha-\gamma$ transition of the RF discharge [33,34]. In this case the electron avalanches develop in the near-electrode sheaths, and with the RF voltage increasing a fast growth of the plasma density within the total discharge gap is observed. According to the opinion of the author of [17], at low pressure the $\alpha-\gamma$ transition curve coincides with such section of the ignition curve of the RF discharge (Paschen branch [35]), that after the breakdown the RF discharge burns at once in γ-regime. However, at low pressure these two criteria do not agree between themselves. Again, visual observations show that at low and intermediate gas pressure the structure of the RF discharge becomes very similar to that of the DC glow discharge when the RF voltage across the electrodes is clearly insufficient to cause the breakdown of near-electrode sheaths. From the current–voltage characteristics of the RF discharge reported in [18] one can also draw a conclusion that lesser values of the RF voltage are required for the discharge to pass from α- to γ- regime with gas pressure decreasing. Therefore, our paper adopted the following change of the RF discharge parameters as a criterion for the passage from α- to γ-regime. Within almost all oxygen pressure range the $\alpha-\gamma$ transition is accompanied by a decrease in the active $I_{rf}\cos(\varphi)$, i.e., the RF voltage value at which the active RF current reaches maximum can be used as a criterion of the start of the $\alpha-\gamma$ transition of the RF discharge. Simultaneously, the $\alpha-\gamma$ transition is accompanied by the rebuilding of the discharge structure: the uniform glow of the positive column characterizing α-regime is transformed into two negative glows and two Faraday spaces overlapping at the centre of the discharge gap at low oxygen pressure. Visual observations clearly register the start of this rebuilding of the discharge structure and the appearance of the dark region at the discharge centre. The discharge glow near the boundaries of near-electrode sheaths also experiences changes: the white glow in α-regime acquires a violet tint during the $\alpha-\gamma$ transition and in γ-regime indicating the appearance of fast electrons in the discharge.

Fig. 3 shows the smallest RF voltages for discharge burning (extinguishing curve) 1 and the largest RF voltages for the weak-current regime to exist (start curve of the $\alpha-\gamma$ transition) 2 against the oxygen pressure. It is clear from the figure that at the oxygen pressures $p > 700$ Pa the $\alpha-\gamma$ transition curve approaches the extinguishing curve of the RF discharge. As is known [16,32], the region of stable existence of weak-current regime of the RF discharge is limited from the moderate

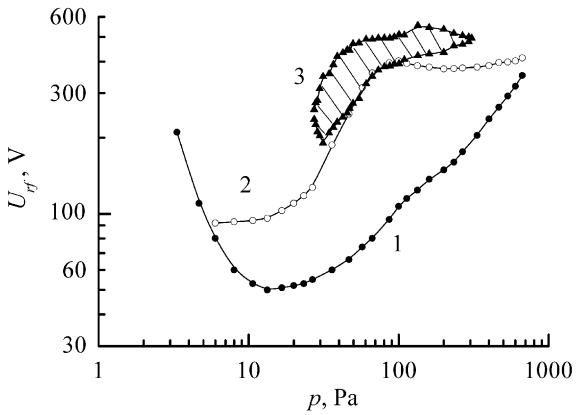

Fig. 3. Extinguishing curve of the RF discharge (1), the alpha-gamma transition curve (2) and the region where the RF oscillations exist (shaded region bounded by solid triangles) 3.

pressure side ($p \sim 1000$ Pa), i.e., for a fixed inter-electrode distance there exists a pressure value p_{cr}, such that for the pressures $p \geqslant p_{cr}$ the RF discharge can exist only in the strong-current regime. On decreasing the pressure, the RF voltage across the electrodes $U_{\alpha-\gamma}$, at which the $\alpha-\gamma$ transition is observed first decreases and reaches a minimum (similar to a minimum at the ignition curve of the DC glow discharge). Then $U_{\alpha-\gamma}$, increases a little and at the oxygen pressure $p \approx 90-100$ Pa reaches a maximum. Then similar to the RF discharge in argon [18], the further decrease in the oxygen pressure leads to a fast decrease of $U_{\alpha-\gamma}$, and in the pressure range $p \leqslant 5$ Pa the $\alpha-\gamma$ transition curve coincides with the extinguishing curve of the RF discharge. Thus the range where the weak-current RF capacitive discharge exists is limited not only from the medium pressure side but also from the low-pressure one. At $p \leqslant 5$ Pa the RF discharge can exist only in the strong-current regime.

Fig. 3 also shows the region of existence of low-frequency oscillations (shaded region 3, limited with triangles). Within the pressure range $p \approx 27-133$ Pa the lower boundary of this region practically coincides with the $\alpha-\gamma$ transition curve, i.e., the oscillations in the RF discharge appear just below the $\alpha-\gamma$ transition curve. In the weak-current regime the RF discharge appears visually as a column of uniform glow occupying the total cross section of the discharge tube between the boundaries of darker near-electrode sheaths. Under the $\alpha-\gamma$ transition the structure of the RF discharge experiences changes: on growing the RF voltage the glow becomes brighter at the boundaries of near-electrode sheaths, and in the central region the glow fades gradually. At the same time, the probe records the low-frequency oscillations of the plasma potential (see Fig. 4).

Within the oxygen pressure range $p \approx 133-307$ Pa with the increase of the RF voltage at the start of the $\alpha-\gamma$ transition the uniform glow is splitting into three distinctly expressed separate glowing regions: two of them are near the boundaries of near-electrode regions, and the third one is in the central part of the discharge. The central glow is similar to the positive column of the DC discharge, and the darker regions between it and the glows located near the boundaries of

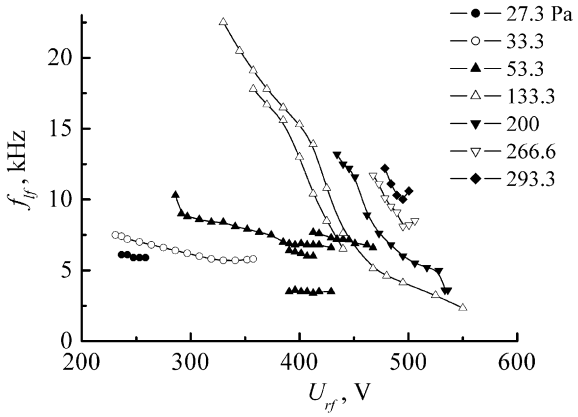

Fig. 4. Plasma potential oscillation frequency at the discharge centre against RF voltage at different oxygen pressure values.

sheaths are similar to the dark Faraday spaces. The low-frequency oscillations do not appear in this range of RF voltages. On increasing the RF voltage further, the intensity of the glow in the central part decreases, and then this glow disappears. The low-frequency oscillations in the central part of the discharge are observed just in this range of RF voltages. Therefore within the pressure range $p \approx 133-307$ Pa the lower boundary of the shaded region (Fig. 3) of the existence of oscillations is above the $\alpha-\gamma$ transition curve. After the RF discharge has experienced the transition into the strong-current regime, the low-frequency oscillations disappear.

Fig. 5 shows the spectra of low-frequency oscillations generated at the RF discharge centre. It is clearly seen from the picture that an increase in the RF voltage leads to the decrease of the oscillation frequency. The oscillation amplitude was in the range of 1–5 V. The oscilloscope pictures of the probe signal also indicate that these oscillations possess a relaxation-like and not a harmonic pattern, their wavelength exceeding several times the inter-electrode distance. Therefore we cannot construct a dispersion law for these oscillations.

Let us consider the processes taking place when the RF discharge is passing from α- to γ-regime at various oxygen pressure values. At low pressure $p < 5$ Pa secondary electrons, having emerged from the electrode surface under bombardment by ions,

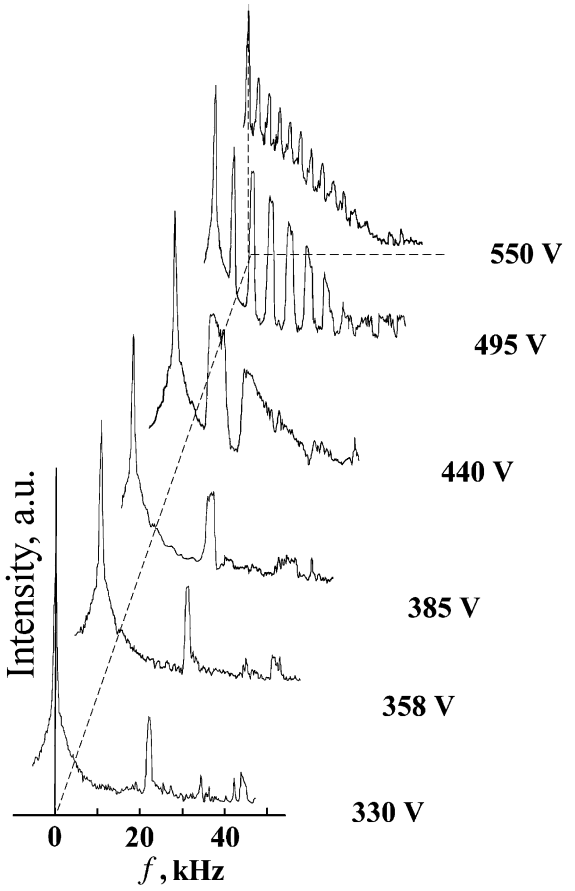

Fig. 5. LF oscillation spectra of plasma potential at the RF discharge centre with the oxygen pressure $p = 133$ Pa and different RF voltage values.

metastable atoms and photons, traverse the near-electrode sheaths actually without collisions acquiring over its width the energy up to $\varepsilon_e \approx eU_{sh}$ (where U_{sh} is the RF voltage drop across the sheath). When $U_{sh} \geqslant U_i$ (U_i is the ionisation potential of the oxygen molecule via electron impact), a beam of fast electrons emerges from the sheath and penetrates the plasma, these electrons being capable to ionise gas molecules along their track. The RF discharge experiences transition to the γ-regime, the characteristics of the quasineutral plasma become similar to two negative glows of the DC discharge overlapping at the discharge centre. When the oxygen pressure is sufficiently small, RF discharge can burn only in the γ-regime, because the voltage drop across the near-electrode sheath exceeds the ionisation potential of gas molecules in the whole region of discharge existence.

At higher pressure secondary electrons traversing the near-electrode sheath have an opportunity to experience one or several elastic or inelastic collisions what results in lesser energy acquired by them over the sheath width compared with the case without collisions. Therefore, with pressure increasing the α–γ transition occurs at higher RF voltage values. At pressure values $p > 100$ Pa the characteristics of the α–γ transition are similar to the ignition of the DC glow discharge: the near-electrode sheath is in the pre-breakdown state, the α–γ transition curve is similar to a Paschen curve [18,32,34].

Let us check whether the breakdown criterion for the near-electrode sheath is met. We will assume the RF electric field E to drop linearly on the way from the electrode surface to the sheath boundary

$$E(x) = \frac{2U_{sh}}{d}\left(1 - \frac{x}{d}\right), \tag{1}$$

where d is the thickness of the near-electrode sheath, $x = 0$ at the surface of the electrode. As the electric field is not constant within the sheath, we should write the breakdown criterion for the sheath in the following form:

$$\gamma\left[\exp\left(\int_0^d \alpha\,\mathrm{d}x\right) - 1\right] = \mu = 1, \tag{2}$$

where γ is the coefficient of the secondary ion–electron emission from the electrode surface, α is the first Townsend's coefficient. We can employ for α the following approximate formula:

$$\alpha = Ap\exp\left(-\frac{B}{E(x)/p}\right), \tag{3}$$

where in the case of strong fields $E/p > 150$ V/(cm Torr) for oxygen $A = 22.5\ \mathrm{Torr}^{-1}\,\mathrm{cm}^{-1}$ and $B = 340$ V/(cm Torr). Let us first evaluate the coefficient γ. At oxygen pressure of 1 Torr (133 Pa), measured thickness of the near-electrode sheath of 3 mm and the RF voltage value of

$U_{\alpha\gamma} = 385$ V for the start of the $\alpha-\gamma$ transition the sheath breakdown criterion (2) is met if $\gamma \approx 0.011$. Then for same value of the coefficient γ, the sheath thickness of 5 mm, the oxygen pressure of 0.1 Torr (13.3 Pa) and the RF voltage value $U_{\alpha\gamma} = 96$ V the coefficient $\mu = 2.4 \cdot 10^{-3} \ll 1$, i.e., the criterion for breakdown of the near-electrode sheath (2) for the $\alpha-\gamma$ transition of the RF discharge in low-pressure oxygen is not met. Generally, under these conditions we did not manage to find the value of the RF voltage in the range below 10 kV, at which $\mu = 1$; even with the 10-fold increase of the quantity γ, in any case we have $\mu \ll 1$. Breakdown curves of the DC discharge in oxygen possess a minimum at $pd_{\min} \approx 56$ Pa cm (0.42 Torr cm) and $U_{\min} \approx 415$ V [36]. The minimum of the $\alpha-\gamma$ transition curve (Fig. 3) possesses the coordinates $p_{\min} \approx 200$ Pa (1.5 Torr) and $U_{\alpha\gamma.\min} \approx 374$ V. For the measured sheath thickness $d \approx 0.25$ cm the value of the product is $pd = 50.7$ Pa cm (0.38 Torr cm), what is in good agreement with the data for the DC breakdown. Therefore we can conclude that at oxygen pressure of $p > 100$ Pa the $\alpha-\gamma$ transition is indeed accompanied by the breakdown of the near-electrode sheath. However at $pd_{\min} = 0.05$ Torr cm (6.65 Pa cm) large voltage values $U_{\alpha\gamma} \gg 1000$ V are required for the breakdown of the near-electrode sheath [36]. Consequently, at low gas pressure $p < 60$ Pa the near-electrode sheath of the RF discharge is not broken down, but is a source of beams of fast electrons.

As was shown in paper [13], attachment-induced ionisation instability can be excited in the RF-capacitive discharge in oxygen. In the RF discharge in oxygen there are a large number of negative ions O^-, whose concentration can be comparable to or even can exceed the concentration of electrons [7,8]. The attachment-induced ionisation instability was theoretically treated in papers [21–23]. Here is the necessary condition for the onset of this instability

$$\frac{k_a k_a^*}{k_i k_i^*} > 1, \tag{4}$$

where $k^* = (T_e/k)(\partial k/\partial T_e)$, k_a and k_i are the attachment and ionisation coefficients. Condition (4) can be rewritten in a simplified form

$$\frac{\partial k_a/\partial T_e}{\partial k_i/\partial T_e} > 1. \tag{5}$$

The coefficient k_a of electron attachment must increase with the electron temperature T_e growing. When condition (5) is met, electron losses due to attachment to oxygen molecules dominate over electron generation due to ionisation during the positive fluctuation of the electron temperature.

Let us check the fulfillment of criterion (5) under conditions of our experiments when LF oscillations are observed in the RF discharge. With the help of the Bolsig code from Kinema Software [37] we obtained the ionisation rate ν_i of and attachment rate ν_a to oxygen molecules against electron temperature T_e (Fig. 6). Using $\nu_i = k_i N_g$ and $\nu_a = k_a N_g$, where N_g is the concentration of oxygen molecules, we have

$$R = \frac{\partial \nu_a/\partial T_e}{\partial \nu_i/\partial T_e} = \frac{\partial k_a/\partial T_e}{\partial k_i/\partial T_e}. \tag{6}$$

The quantity R is also presented in Fig. 6. It is clear from Fig. 6, that $R > 1$ in the range of electron temperature values $T_e < 2.6$ eV, i.e., the attachment-induced ionisation instability can occur only at low electron temperature.

Fig. 7 depicts the electron temperature T_e we have measured at the RF discharge centre against the RF voltage applied. It is clear from this figure that in the weak-current regime of the RF

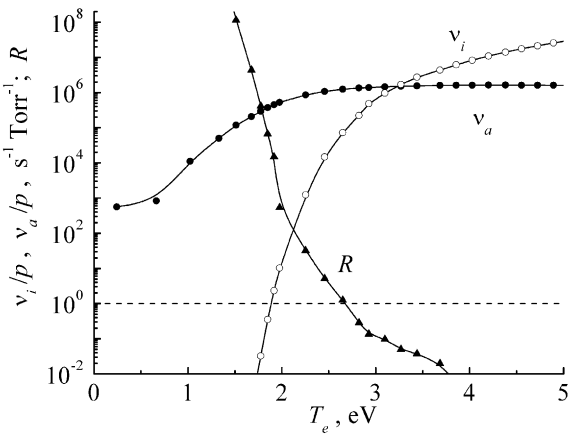

Fig. 6. Ionisation ν_i and attachment ν_a rates as well as the quantity R against electron temperature T_e.

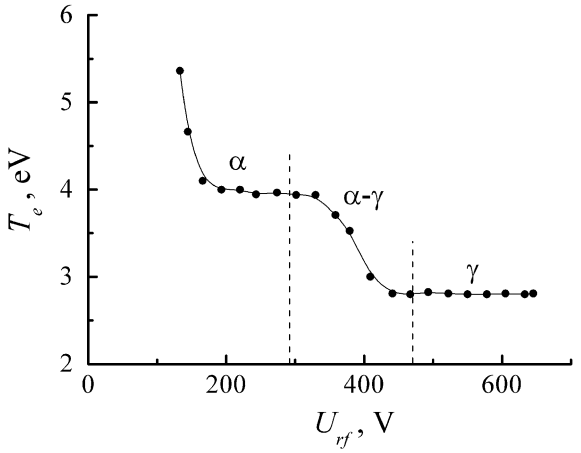

Fig. 7. Electron temperature at the discharge centre against RF voltage at the oxygen pressure $p = 53.3$ Pa.

discharge the electron temperature is almost constant and is equal to about 4 eV (excluding the region of lower RF voltage values near the potential of the discharge extinguishing). For the $\alpha-\gamma$ transition we observe the uniform decrease in electron temperature with the increase of the RF voltage. In the strong-current regime T_e remains approximately constant and equals to 2.8 eV. Consequently, in the total range of RF voltages studied the quantity $R<1$, criterion (5) is not met, therefore the LF oscillations we have observed cannot be associated with the attachment-induced ionisation instability.

Fig. 8 shows the axial profiles of the plasma density n_i for the oxygen pressure values of 13.3 and 133 Pa. At low oxygen pressure (13.3 Pa, Fig. 8a) the profiles of the plasma density have a bell-shaped form in the total range of RF voltages under study; the plasma density increases uniformly with the RF voltage increasing. At higher pressure (133 Pa, Fig. 8b) in the weak-current regime of burning with the increase of the RF voltage the plasma density at the discharge centre increases, under the α–γ transition the growth rate of the plasma density decreases noticeably (in a number of cases the plasma density remained practically constant and even decreased a little under the transition from the α- to the γ-regime), and in the γ-regime the increase in the RF voltage leads to a fast increase in the plasma density.

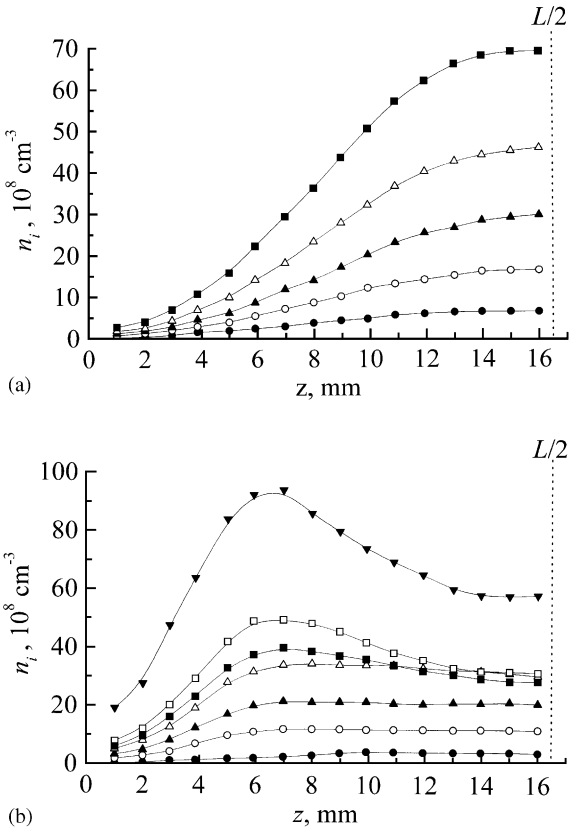

Fig. 8. Axial profiles (from the electrode to the discharge centre) of the plasma density at the pressure values 13.3 Pa (a) and 133 Pa (b) and the applied RF voltage values: (a) (1) 110 V; (2) 220; (3) 330; (4) 440; (5) 550 V. (b) (1) 110 V; (2) 220; (3) 330; (4) 440; (5) 495; (6) 550; (7) 660 V.

Let us now consider the processes occurring during the α–γ transition of the RF discharge that can lead to the generation of LF oscillations. Let us ignite the discharge in a weak-current regime and reach the start of the $\alpha-\gamma$ transition by increasing the RF voltage. The RF voltage drop across the sheath becomes sufficiently large to let a beam of electrons with enhanced energy emerge from the sheath. This electron beam makes easier the transport of the discharge current; therefore the RF field in the quasineutral plasma E_{pl} decreases a little. The electron temperature T_e also decreases. This, in its turn, leads to a small decrease of the attachment rate ν_a of electrons to oxygen molecules and to a noticeable decrease of

the ionisation rate ν_i of molecules by plasma electrons (it follows from Figs. 6 and 7, that during the $\alpha-\gamma$ transition the temperature T_e decreases from 4 to 2.9 eV, whereas ν_a decreases by 15%, and ν_i by 17-fold). The decrease in the RF field in plasma causes the decrease of the near-electrode sheath thickness and the increase of the RF voltage drop across the sheath. The energy and number of fast electrons in the beam emerging from the sheath increases thus lowering the RF field in plasma further.

But the number of fast electrons in this beam capable of ionising gas molecules is still small. The lowering of the RF field in plasma is accompanied by the loss of charged particles (electron attachment to oxygen molecules, recombination of electrons and negative ions with positive ions, ambipolar diffusion to the walls and electrodes of the discharge chamber). Therefore, the density of the quasineutral plasma lowers in time. Some lowering of the density in the central part of the discharge under the $\alpha-\gamma$ transition is clear from Fig. 8b.

Starting to decay, the plasma becomes incapable of transporting the discharge current; therefore the RF field in the plasma increases. This leads to the increase in the near-electrode sheath thickness and to the decrease of the RF voltage drop across it. The conditions for the formation of the beam of fast electrons within the sheath deteriorate. The plasma density in the central region increases to its initial value due to the increased ionisation by plasma electrons. But the increased plasma density involves the decrease of the near-electrode sheath thickness. The sheaths again become the source of fast electrons, and the process repeats itself.

Actually during the $\alpha-\gamma$ transition the RF discharge is passing from one unstable state A (whose characteristics are closer to ones of the weak-current regime) to another unstable state B (closer to the strong-current regime). The state A is unstable because of the appearance of the beams of fast electrons in the sheaths, and state B is unstable because these beams are unable to provide a sufficiently high ionisation rate in the quasineutral plasma. This transition of the RF discharge from state A to state B and back gives rise to oscillations of the RF voltage across the electrodes, of the RF current as well as of the plasma potential. The low frequency of these oscillations (of kilohertz range, Fig. 4) points to the dominant role of slow processes under these conditions (recombination, diffusion), leading to the loss of charged particles in the plasma.

At the sufficiently large RF voltage the beams of fast electrons ensure the high rate of ionisation in the quasi-neutral plasma. This ionisation, as well as the diffusion of charged particles near the boundaries of the sheaths compensates the losses of electrons and ions in the central part of the discharge due to recombination and diffusion. The discharge becomes stable and continues to burn in the strong-current regime, and low-frequency oscillations disappear.

Conclusions

Thus in the present work are reported the recorded current–voltage characteristics of the capacitive RF discharge in oxygen, the extinguishing curve of the discharge and the α–γ transition curve, electron temperature and axial profiles of the plasma density. It is shown that in a certain range of oxygen pressures the $\alpha-\gamma$ transition is accompanied by low-frequency oscillations of the plasma potential in the kilohertz frequency range. It is obtained that the region of existence of the weak-current regime of the RF-capacitive discharge is limited not only from the medium pressure side, but also from the low-pressure one.

References

[1] Steinbruchel C, Curtis BJ, Lehmann HW, Widmer R. IEEE Trans Plasma Sci 1986;14:137.
[2] Nakano J, Suzuki M. Vacuum 1986;36:85.
[3] Atanassova ED, Toncheva LT. Thin Solid Films 1986;137:235.
[4] Hope DAO, Cox TI, Deshmukh VGI. Vacuum 1987;37:275.
[5] Jurgensen CW. J Appl Phys 1988;64:590.
[6] Lichtenberg AJ, Vahedi V, Lieberman MA, Rognlien T. J Appl Phys 1994;75:2339.
[7] Stoffels E, Stoffels WW, Vender D, Kando M, Kroesen GMW, de Hoog FJ. Phys Rev E 1995;51:2425.

[8] Vender D, Stoffels WW, Stoffels E, Kroesen GMW, de Hoog FJ. Phys Rev E 1995;51:2436.
[9] Feoktistov VA, Mukhovatova AV, Popov AM, Rahimova TV. J Phys D 1995;28:1346.
[10] Aoyagi K, Ishikawa I, Saito Y, Suganomata S. Jpn J Appl Phys 1996;35:6248.
[11] Aoyagi K, Hirose Y, Ishikawa I, Saito Y, Suganomata S. Jpn J Appl Phys 1997;36:5290.
[12] Shibata M, Nakano N, Makabe T. J Phys D 1998;37:4182.
[13] Katch H-M, Doehlich A, Kawetzki T, Quandt E, Dobele H-F. Appl Phys Lett 1999;75:2023.
[14] Faga K, Kimura T, Ohe K. J Phys D 1997;30:1219.
[15] Morscheidt W, Longo S, Hassouni K, Arefi F, In: Proceedings of XXV International Conference on Phenomena in Ionized Gases, July 17–22, 2001, Vol. 2, Nagoya, Japan, pp. 229.
[16] Raizer YP, Shneider MN, Yatsenko NA. Radio-frequency capacitive discharges. Boca Raton, FL: CRC Press; 1995.
[17] Levitskii SM. Sov Phys Tech Phys 1957;2:887.
[18] Lisovskiy VA. Tech Phys 1998;43:526.
[19] Sabadil H. Beitr Plasmaphys 1968;8:299.
[20] Ishikawa I, Matsumoto M, Suganomata S. J Phys D 1984;17:85.
[21] Haas RA. Phys Rev A 1973;8:1017.
[22] Nighan WL, Wiegand WJ, Haas RA. Appl Phys Lett 1973;22:579.
[23] Nighan WL, Wiegand WJ. Phys Rev A 1974;10:922.
[24] Descoeudres A, Sansonnens L, Hollenstein Ch. Plasma Sources Sci Technol 2003;12:152.
[25] Schulz GJ, Brown SC. Phys Rev 1955;98:1642.
[26] Zakrzewski Z, Kopiczynski T. Plasma Phys 1974;16:1195.
[27] Tichy M, Sicha M, David P, David T. Contrib Plasma Phys 1994;34:59.
[28] Amemiya H. J Phys D 1990;23:999.
[29] Amemiya H. Vacuum 2000;58:100.
[30] Dudin SV. Prib Tekh Exp 1994;4:78 (in Russian).
[31] Lisovskii VA, Yegorenkov VD, Krasnikov OV. Sov Tech Phys Lett 1993;19:701.
[32] Yatsenko NA. Sov Phys Tech Phys 1980;25:1454; Yatsenko NA. Sov Phys Tech Phys 1981;26:678; Yatsenko NA. Sov Phys Tech Phys 1988;33:180.
[33] Godyak VA, Khanneh AS. IEEE Trans Plasma Sci 1986;14PS:112.
[34] Bohm C, Perrin J. J Phys D 1991;24:865.
[35] Lisovskiy VA, Yegorenkov VD. J Phys D 1998;31:3349.
[36] Lisovskiy VA, Yakovin SD, Yegorenkov VD. J Phys D 2000;33:2722.
[37] Pitchford LC, ONeil SV, Rumble JR. Phys Rev A 1981;23:294.